Reconstruction of Coronary Trees from 3DRA Using a 3D+t Statistical Cardiac Prior

Serkan Çimen[1], Corné Hoogendoorn[2], Paul D. Morris[3], Julian Gunn[3], and Alejandro F. Frangi[1]

[1] Center for Computational Imaging & Simulation Technologies in Biomedicine (CISTIB), University of Sheffield, Sheffield, United Kingdom
[2] CISTIB, Universitat Pompeu Fabra and CIBER-BBN, Barcelona, Spain
[3] Department of Cardiovascular Science, University of Sheffield, Sheffield, United Kingdom

Abstract. A 3D+t description of the coronary tree is important for diagnosis of coronary artery disease and therapy planning. In this paper, we propose a method for finding 3D+t points on coronary artery tree given tracked 2D+t point locations in X-ray rotational angiography images. In order to cope with the ill-posedness of the problem, we use a bilinear model of ventricle as a spatio-temporal constraint on the nonrigid structure of the coronary artery. Based on an energy minimization formulation, we estimate i) bilinear model parameters, ii) global rigid transformation between model and X-ray coordinate systems, and iii) correspondences between 2D coronary artery points on X-ray images and 3D points on bilinear model. We validated the algorithm using a software coronary artery phantom.

1 Introduction

Coronary artery disease (CAD) is a serious condition, responsible for almost 1.8 million deaths in the Europe alone [10]. Current clinical practice for interpretation and assessment of the disease still relies on the anatomical information derived from coronary angiography [5]. However, a considerable amount of 3D information of the coronary arteries is lost during 2D projection. It is also hard to study dynamic variation of coronary arteries through 2D projection images [2]. Therefore, providing a clinician with a quantitative 3D+t description of the arterial tree is of utmost importance to aid the diagnosis of CAD and improve therapy planning and catheter-based interventions.

In recent years, a vast amount of research has been carried out to obtain a 3D/3D+t representation of the coronary tree from medical imagery. Among these methods, a class of methods try to build a 3D symbolic model of coronary arteries, which consists of a 3D centerline and, occasionally, the vessel diameter. Most of the modeling based reconstruction methods uses ECG gating to select two or more (4-5) projections from over a hundred images [8,9]. Consequently, a considerable amount of acquired information is discarded by these methods. Additionally, obtaining 3D+t reconstruction via ECG-gated reconstruction methods is a tedious task. This is mainly because 3D reconstructions for different

P. Golland et al. (Eds.): MICCAI 2014, Part II, LNCS 8674, pp. 619–626, 2014.

cardiac phases must be generated separately. However, not all the segments of the coronary arterial tree are visible in all the rotational angiographic views.

In this paper, we propose a novel method to reconstruct 3D+t points of coronary arterial trees from rotational X-ray angiography, which generally constitutes the initial step in a coronary artery reconstruction workflow. Our method uses all the images collected during the angiographic study and outputs the 3D+t points of the coronary arteries by utilizing a spatio-temporal model of the epicardial surface. We validated our method with a software phantom of the left coronary artery tree and a spatio-temporal model of the left ventricular epicardium.

2 Method

Our method assumes that the coronary arteries are attached to and move together with the ventricular epicardium. Therefore, a statistical model of the epicardial surface could implicitly describe the non-rigid structure of coronary arteries if the arterial locations on the model are known. Our method employs a bilinear model of the left ventricle (Section 2.1) as the statistical model.

Given 2D points tracked over sequence of X-ray images, we formulate an energy that consists of two terms: namely, a distance and a regularization term. By minimizing this energy, we find the bilinear model parameters that best describe the observed 2D points. In order to iteratively minimize the energy and estimate the correspondences between 2D coronary artery points obtained from X-ray images and 3D points on the bilinear model of the left ventricle, we adopted an EM-like method, which combines EM with a deterministic annealing scheme [3] (Section 2.2).

2.1 Construction of a Bilinear Ventricle Model

A bilinear statistical model [12] is a natural candidate to model observations, which possess variations due to two independent factors. In [7], it was shown that a bilinear model could provide a way to model the shape of the human heart by separating inter-subject from temporal variations. Here, we constrain shape and motion of the coronary arteries by a bilinear model of the ventricular epicardium, assuming approximate correspondence between 2D coronary points on the X-ray images and 3D epicardial points on the bilinear model.

Suppose our training set consists of temporally and spatially aligned ventricle surfaces of S subjects in C cardiac phases. Each training ventricle surface is represented by N landmark points in a d-dimensional Euclidean space. Those landmark points are concatenated to form $K(= N \times d)$ dimensional observation vector, $\boldsymbol{y}^{sc}$. By using a bilinear model, each element of $\boldsymbol{y}^{sc}$ is written as $y_k^{sc} = \boldsymbol{a}^{s\,T} \boldsymbol{W}_k \boldsymbol{b}^c$. Here, $\boldsymbol{a}^s$, $\boldsymbol{b}^c$ denotes bilinear model parameters of subject and phase, which are I and J dimensional vectors, respectively. $\boldsymbol{W}_k$ is an $I \times J$ matrix determining the interaction of two factors.

Model building is carried out through a training process by which we find parameters, $\boldsymbol{a}^s$, $\boldsymbol{b}^c$, for each subject class s and phase class c and the interaction

matrices, $\boldsymbol{W}_k$'s, by minimizing the total squared error. To this end, we use an efficient iterative method based on SVD [12]. Model training provides $I \times S$ matrix $\boldsymbol{A} = [\boldsymbol{a}^1 \cdots \boldsymbol{a}^S]$, $J \times C$ matrix $\boldsymbol{B} = [\boldsymbol{b}^1 \cdots \boldsymbol{b}^C]$ and $IK \times J$ matrix $\boldsymbol{W}$.

2.2 Energy Formulation and Minimization

We assume that we are given M 2D points ($M \ll N$), which are assumed to lie on the surface of the bilinear model for each of F X-ray images. The corresponding ECG signal is used to assign each X-ray image to a cardiac phase in a canonical cycle. From the time-stamped point set we estimate i) the bilinear model parameters, $\widehat{\boldsymbol{a}}$ and $\widehat{\boldsymbol{B}}$, ii) the rotation matrix and the translation vector between the bilinear model and the X-ray coordinate systems, $\widehat{\boldsymbol{R}}$ and $\widehat{\boldsymbol{t}}$, and iii) the correspondences between the 2D points on the X-ray images and the 3D points on the bilinear model, denoted by a $M \times N$ correspondence matrix $\boldsymbol{G}$.

We consider the problem as a point set alignment problem. Assuming that the projections of the points in the bilinear model of the ventricle specifies Gaussian cluster centers, the distribution of ventricle points could be represented by a Gaussian mixture model (GMM). We find $\widehat{\boldsymbol{a}}$, $\widehat{\boldsymbol{B}}$, $\widehat{\boldsymbol{R}}$, $\widehat{\boldsymbol{t}}$ and $\boldsymbol{G}$ by minimizing a log-posterior energy function. This energy function can be written as the weighted sum of a distance and a regularization term [3].

The distance term measures the sum of squared distances between 2D observations and 2D projections of the bilinear model point estimates. It can be written as

$$E_{dist} = \sum_{m}^{M} \sum_{n}^{N} \sum_{f}^{F} G_{mn} \|\boldsymbol{x}_m^f - \widehat{\boldsymbol{x}}_n^f\|^2 \tag{1}$$

where $\boldsymbol{x}_m^f$ is the mth 2D observation from fth X-ray image and $\widehat{\boldsymbol{x}}_n^f$ is the 2D projection of the 3D bilinear model point estimate, $\widehat{\boldsymbol{y}}_n^f$, which are given as

$$\begin{bmatrix} \widehat{\boldsymbol{x}}_n^f \\ 1 \end{bmatrix} \simeq \boldsymbol{P}^f \begin{bmatrix} \widehat{\boldsymbol{y}}_n^f \\ 1 \end{bmatrix} = \boldsymbol{P}^f \begin{bmatrix} \widehat{\boldsymbol{R}}[\overline{\boldsymbol{W}}^{VT} \widehat{\boldsymbol{a}}]^{VT} \widehat{\boldsymbol{b}} + \widehat{\boldsymbol{t}} \\ 1 \end{bmatrix} \tag{2}$$

where $\boldsymbol{P}^f$ is the projection matrix, which is extracted from X-ray image tags and superscript VT denotes vector tranpose operation [12]. Note in the above equation $\overline{\boldsymbol{W}}$ is a $3I \times J$ matrix made of the rows of $\boldsymbol{W}$, which corresponds to one of the landmark point. It is also important to note that $\widehat{\boldsymbol{b}}$ given above is the column of $\widehat{\boldsymbol{B}}$ corresponding to the phase of fth X-ray image. When the phase of an X-ray image does not coincide with the discrete cardiac phases of the bilinear model training set, we form point estimates at two neighboring discrete time points and linearly interpolate to find $\widehat{\boldsymbol{y}}_n^f$.

The regularization term is defined as the negative log-likelihood of the prior distribution of bilinear model parameters. To this end, the bilinear model parameters, which are learned during training are used to perform kernel density estimations of the components of the parameter vector $\boldsymbol{a}^s$ and matrix $\boldsymbol{B}$. The regularization term can be written as

$$E_{reg} = \begin{cases} -\sum_{i=1}^{I} \log\left(\frac{1}{hS}\sum_{s=1}^{S} k\left(\frac{\widehat{a}_i - a_i^s}{h}\right)\right) & \text{if minimizing for } \widehat{\boldsymbol{a}}, \widehat{\boldsymbol{R}}, \widehat{\boldsymbol{t}} \\ -\sum_{j=1}^{J}\sum_{c=1}^{C} \log\left(\frac{1}{hC}\sum_{\bar{c}=1}^{C} k\left(\frac{\widehat{B}_{jc} - b_j^{\bar{c}}}{h}\right)\right) & \text{if minimizing for } \widehat{\boldsymbol{B}} \end{cases} \tag{3}$$

where h denotes the bandwidth and $k(\cdot)$ is a Gaussian kernel.

Finally, total energy to minimize is written as

$$E_{tot} = E_{dist} + \tau\lambda E_{reg} \tag{4}$$

where λ determines the weighting between two energy terms and τ is the annealing parameter.

We adopted an EM-like method [3] to find the bilinear model parameters, transformation and correspondences by an alternating scheme. The EM-like method combines the EM algorithm with a deterministic annealing scheme. Compared to the EM algorithm, we do not estimate covariance matrices for Gaussian cluster. Instead, we use an annealing parameter to decrease the isotropic variance of the Gaussian clusters in every iteration.

Since the probability of corresponding to an artery point is not equal for each landmark point, we used different mixing coefficients, p_n, for Gaussian clusters. We used the coronary arteries from an atlas of the human heart [6] to determine p_n for every landmark of the bilinear model. Because the same atlas was used to generate the bilinear model training data, correspondences of landmark points between the atlas segmentation and bilinear model are known. We determine the points on the surface of the atlas segmentation that are closest to the centerlines of the segmented coronary arteries. Using these closest points, we find a signed distance function on the atlas segmentation and assign p_n values according to $p_n = \frac{\exp^{-(d_n/\zeta)^2}}{\sum_{n=1}^{N}\exp^{-(d_n/\zeta)^2}}$, where d_n is the distance of nth landmark to the nearest point and ζ is a constant. A large ζ value avoids strict correspondences due to p_n values and provides robustness against the anatomical variability.

In order to cope with the outlier data points, we used two outlier rejection strategies. First, we model the outlier observation points by adding a uniform distribution to the mixture model with a weight, w. Second, we discard the projected bilinear model points and the corresponding Gaussian cluster if the sum of the membership probabilities for all the M observed points are smaller than a threshold, β.

The algorithm can be simply described as follows: In the E step, we update the entries of the correspondence matrix, $\boldsymbol{G}$, using the membership probabilities

$$G_{mn} = \left(p_n \exp\left(-\frac{\|\boldsymbol{x_m^f} - \widehat{\boldsymbol{x}}_{\boldsymbol{n}}^{\boldsymbol{f}}\|^2}{2\tau F}\right)\right) \Big/ \left(c + \sum_{n=1}^{N} p_n \exp\left(-\frac{\|\boldsymbol{x_m^f} - \widehat{\boldsymbol{x}}_{\boldsymbol{n}}^{\boldsymbol{f}}\|^2}{2\tau F}\right)\right) \tag{5}$$

where p_n denote the mixing coefficient for the nth Gaussian cluster, τ is the annealing parameter and constant c is given by $\frac{w}{1-w}\frac{\sqrt{2\Pi\tau}}{M}$. In the M step, we minimize the total energy (Equation 4). The overall algorithm is given in Algorithm 1.

Algorithm 1. 3D+t Coronary Artery Reconstruction Algorithm

Input: 2D points tracked over X-ray sequence, projection matrices, initial transformation ($\boldsymbol{R_{ini}}$, $\boldsymbol{t_{ini}}$), initial parameters for the bilinear ventricle model ($\boldsymbol{a_{ini}}, \boldsymbol{B_{ini}}$), annealing parameters (τ_{ini}, τ_{up} and τ_{fin}) and other parameters (λ, β and ζ)

Output: Estimates for bilinear model parameters ($\widehat{\boldsymbol{a}}, \widehat{\boldsymbol{B}}$), global transformation ($\widehat{\boldsymbol{R}}, \widehat{\boldsymbol{t}}$) and correspondence matrix ($\boldsymbol{G}$)

$\widehat{\boldsymbol{R}} \leftarrow \boldsymbol{R_{ini}}$, $\widehat{\boldsymbol{t}} \leftarrow \boldsymbol{t_{ini}}$, $\widehat{\boldsymbol{a}} \leftarrow \boldsymbol{a_{ini}}$, $\widehat{\boldsymbol{B}} \leftarrow \boldsymbol{B_{ini}}$ and $\tau \leftarrow \tau_{ini}$
repeat
  Compute $\boldsymbol{G}$ (Equation 5)
  if $\sum_{m=1}^{M} G_{mn} < \beta$ **then**
    Discard $\widehat{\boldsymbol{x}}_n^f$, and its Gaussian cluster
  end if
  Update $\widehat{\boldsymbol{R}}$, $\widehat{\boldsymbol{t}}$, and $\widehat{\boldsymbol{a}}$ by minimizing E_{tot} (Equation 4)
  Update $\widehat{\boldsymbol{B}}$ by minimizing E_{tot} (Equation 4)
  $\tau \leftarrow \tau_{up} \times \tau$
until $\tau < \tau_{fin}$

3 Experiments and Results

Training surface meshes describing the left ventricular epicardium ($N = 2044$) are obtained using an atlas based segmentation algorithm [6] from 134 retrospectively ECG-gated multi-slice CT images. These meshes are temporally aligned as in [7] to compensate for heart rate differences between patients. Procrustes alignment [4] is performed to align training surfaces spatially. During Procrustes alignment, we opted for rigid transformations without scaling and incorporated the scaling effects into our statistical model.

In order to quantitatively evaluate our algorithm, we generated synthetic rotational angiography data using the single left coronary artery geometry of the 4D XCAT phantom [11]. The cardiac cycle was set to be 1000ms, with no respiratory motion present. X-ray imaging parameters, including projection matrices, number of images (117) and frame rate (30 fps) were derived from a clinical dataset. Since we have the 4D ground truth information for the centerlines, we created a total of 208 corresponding coronary artery points (one center point for each longitudinal knot of non-uniform rational B-spline surface [11]) and projected these to generate the 2D observation points in 117 projection images.

We used the phantom data to evaluate the algorithm's robustness to missing data and noise. In the first experiment (*Experiment 1*), we randomly removed 0% to 50% of 2D observation points which describe the projected 2D trajectory of each tracked coronary artery point along the sequence of projection images. In the second experiment (*Experiment 2*), we removed the 2D observation points according to a sampling scheme that mimics the sparsity associated to missing detail in the detection of centerline points in the 2D views. To this end, we selected a set of points, $\mathcal{P}_1$, which consisted of a starting point, bifurcations and end points. Similarly, we defined $\mathcal{P}_2$ as the set of points, which are the midpoints of the segments described by the points in the set $\mathcal{P}_1$ and defined $\mathcal{P}_3$ as the set

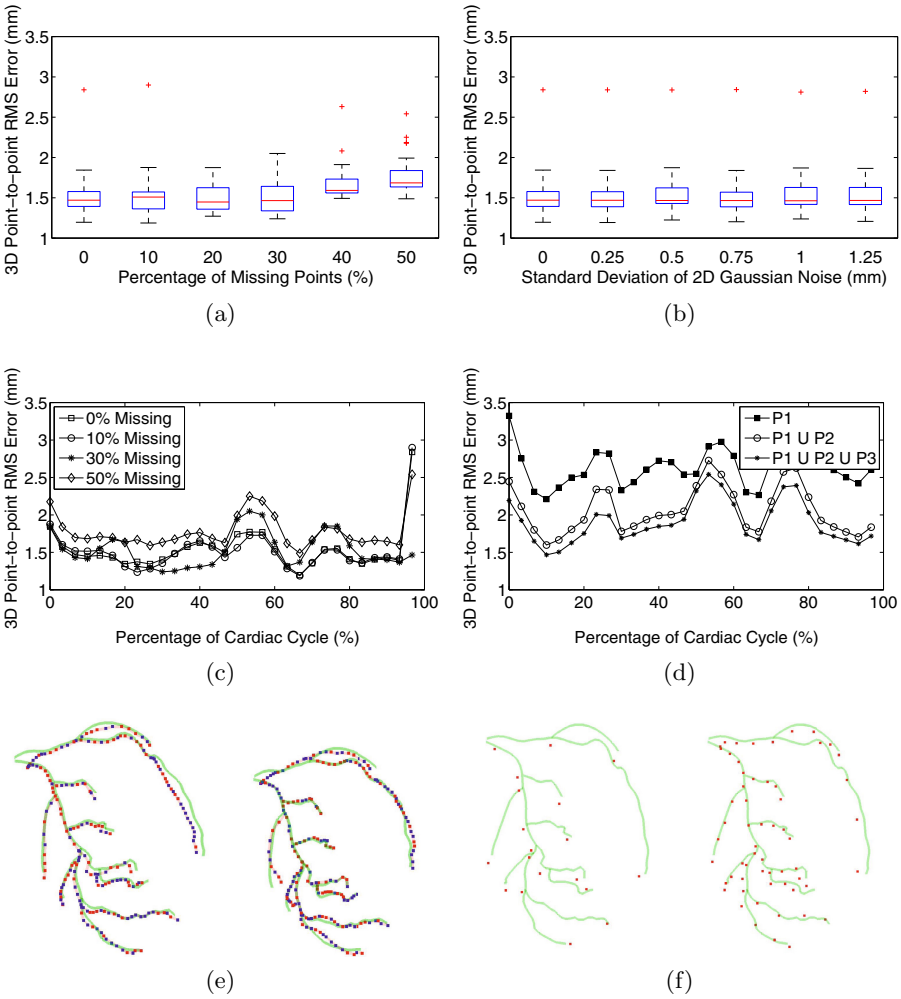

Fig. 1. 3D+t reconstruction results on phantom data. See text for the details of the experiments. (a) Results of the *Experiment 1*, (b) results of the *Experiment 3*, (c) results of the *Experiment 1* for all cardiac phases, (d) results of the *Experiment 2* for all cardiac phases , (e) qualitative results of the *Experiment 1* for end-diastolic and end-systolic phases, (f) qualitative results of the *Experiment 2* for $\mathcal{P}_1$ and $\mathcal{P}_1 \cup \mathcal{P}_2 \cup \mathcal{P}_3$. For the qualitative results, the ground truth centerline of the coronary artery tree is shown in green. Reconstructed points are given in red if 2D observation is available in the corresponding image and in blue if the 2D observation is removed.

of points, which are the midpoints of the segments described by the points in the set $\mathcal{P}_1$ and $\mathcal{P}_2$. We applied our reconstruction algorithm given the points in the sets $\mathcal{P}_1$ (9.13% of all points), $\mathcal{P}_1 \cup \mathcal{P}_1$ (16.35% of all points) and $\mathcal{P}_1 \cup \mathcal{P}_2 \cup \mathcal{P}_3$ (28.37% of all points). We also evaluated the performance under uncertain

measurements by adding zero mean Gaussian noise (σ 0.25 to 1.25 mm) to the 2D points (*Experiment 3*). In all of the experiments, the reconstruction errors were measured as the root-mean-square errors in 3D between the reconstructed points and the true 3D positions.

The parameters of the algorithm are set empirically. The annealing parameters, τ_{ini}, τ_{fin} and τ_{up} were set to 500, 3 and 0.95, respectively (cf. [3] for details). The threshold for rejecting projected bilinear point, β, was set to 0.05 and the weighting, λ, of the regularization term was set to 2.5×10^5. Finally, the weight for the uniform outlier cluster in the GMM, w, was set to 1.0×10^{-8} since we assume that there are no outliers in 2D observations.

The results show that the 3D+t reconstruction performance of our algorithm stays stable even under 1.25 mm 2D observation noise, which is approximately 6-7 times of the pixel resolution of the rotational angiography (Figure 1(b)).

Although there are some outliers, the results indicate that the proposed method is able to handle missing data (Figure 1(a)). In particular, the qualitative results shows that the 3D reconstruction of missing data points are recovered satisfactorily. There are two sources of the outliers. First, the method is not able to accurately reconstruct the points near the LAD-LCX branching. It is possible that this region could not be modeled solely by the left ventricular epicardium. Second, the algorithm returned suboptimal results for the phase related bilinear model parameters, which affects its performance in some cardiac phases. This could be related to our current stopping criteria and requires further experiments.

The accuracy of the algorithm quickly increases with addition of a small number of points to the base set, $\mathcal{P}_1$ and continue to increase as more 2D observations points are added (Figure 1(d)).

4 Conclusion

In this paper, we present a method to reconstruct the 3D+t points of the coronary tree from rotational angiography images. The regularization is achieved by constraining the motion and the shape of the coronary arteries by a spatio-temporal model of the epicardial surface of the ventricle. Although it is not discussed in this paper, the reconstructed 3D+t points could be converted to 3D+t centerlines by a linking procedure [9] or 3D+t vascular surface [13] by incorporating the radius information.

Currently, we assume that the 2D points tracked over the sequence of X-ray images are provided. However, automatic methods to determine the point correspondences must be explored.

A temporal mapping between the cardiac cycle of the bilinear model and the angiography images is required to consider the mismatch of cardiac phases due to heart rate differences. A simple solution would be to employ a piecewise linear mapping function [1].

Our method assumes that the angiography images are collected during a breath hold. To overcome this drawback, a respiratory motion model could be

incorporated into the energy minimization formulation at the expense of estimating more parameters.

References

1. Baka, N., Metz, C.T., Schultz, C., Neefjes, L., van Geuns, R.J., Lelieveldt, B.P.F., Niessen, W.J., van Walsum, T., de Bruijne, M.: Statistical coronary motion models for 2D+t/3D registration of x-ray coronary angiography and CTA. Med. Image Anal. 17(6), 698–709 (2013)
2. Chen, S.Y.J., Carroll, J.D.: Kinematic and deformation analysis of 4-D coronary arterial trees reconstructed from cine angiograms. IEEE Trans. Med. Imaging 22(6), 710–721 (2003)
3. Chui, H., Rangarajan, A.: A feature registration framework using mixture models. In: IEEE Workshop MMBIA, pp. 190–197 (2000)
4. Goodall, C.: Procrustes methods in the statistical analysis of shape. J. R. Stat. Soc. Series B Stat. Methodol. 53(2), 285–339 (1991)
5. Grech, M., Debono, J., Xuereb, R.G., Fenech, A., Grech, V.: A comparison between dual axis rotational coronary angiography and conventional coronary angiography. Catheter. Cardiovasc. Interv. 80(4), 576–580 (2012)
6. Hoogendoorn, C., Duchateau, N., Sanchez-Quintana, D., Whitmarsh, T., Sukno, F.M., De Craene, M., Lekadir, K., Frangi, A.F.: A high-resolution atlas and statistical model of the human heart from multislice CT. IEEE Trans. Med. Imaging 32(1), 28–44 (2013)
7. Hoogendoorn, C., Sukno, F.M., Ordás, S., Frangi, A.F.: Bilinear models for spatio-temporal point distribution analysis. Int. J. Comput. Vis. 85(3), 237–252 (2009)
8. Jandt, U., Schäfer, D., Grass, M., Rasche, V.: Automatic generation of 3D coronary artery centerlines using rotational x-ray angiography. Med. Image Anal. 13(6), 846–858 (2009)
9. Liao, R., Luc, D., Sun, Y., Kirchberg, K.: 3-D reconstruction of the coronary artery tree from multiple views of a rotational x-ray angiography. Int. J. Cardiovasc. Imaging 26, 733–749 (2010)
10. Nichols, M., Townsend, N., Scarborough, P., Rayner, M.: Cardiovascular disease in europe: epidemiological update. Eur. Heart. J. 34(39), 3028–3034 (2013)
11. Segars, W.P., Sturgeon, G., Mendonca, S., Grimes, J., Tsui, B.M.W.: 4D XCAT phantom for multimodality imaging research. Med. Phys. 37(9), 4902–4915 (2010)
12. Tenenbaum, J.B., Freeman, W.T.: Separating style and content with bilinear models. Neural. Comput. 12(6), 1247–1283 (2000)
13. Yang, J., Wang, Y., Liu, Y., Tang, S., Chen, W.: Novel approach for 3-D reconstruction of coronary arteries from two uncalibrated angiographic images. IEEE Trans. Image Process. 18(7), 1563–1572 (2009)